Title

Chaperone mediated coupling of subunit availability to activation of flagellar Type III Secretion

Authors

Owain J. Bryant[a], Betty Y-W. Chung[a] and Gillian M. Fraser[a,1]

Affiliations

[a]Department of Pathology, University of Cambridge, Tennis Court Road, Cambridge, CB2 1QP, United Kingdom.

Corresponding author

[1]Gillian M. Fraser

Department of Pathology, University of Cambridge, Tennis Court Road, Cambridge, CB2 1QP, United Kingdom.

Phone: +44 1223 330245

Email: gmf25@cam.ac.uk

Abstract

Bacterial flagellar subunits are exported across the cell membrane by the flagellar Type III Secretion System (fT3SS), powered by the proton motive force (pmf) and a specialized ATPase that enables the flagellar export gate to utilise the pmf electric potential (ΔΨ). Export gate activation is mediated by the ATPase stalk, FliJ, but how this process is regulated to prevent wasteful dissipation of pmf in the absence of subunit cargo is not known. Here, we show that FliJ activation of the export gate is regulated by flagellar export chaperones. FliJ binds unladen chaperones and, using novel chaperone variants specifically defective for FliJ binding, we show that disruption of this interaction attenuates motility and cognate subunit export. We demonstrate *in vitro* that chaperones and the FlhA export gate component compete for binding to FliJ, and show *in vivo* that unladen chaperones, which would be present in the cell when subunit levels are low, sequester FliJ to prevent activation of the export gate and attenuate subunit export. Our data indicate a mechanism whereby chaperones couple availability of subunit cargo to pmf-driven export by the fT3SS.

Keywords

bacterial flagella biogenesis; Type III Secretion System; proton motive force; protein export

Abbreviations

Type III secretion system (T3SS); flagellar Type III secretion system (fT3SS); virulenceType III secretion system (vT3SS); proton motive force (pmf)

45 **Introduction**

46 Bacterial flagella are large macromolecular rotary motors that enable cell motility. In
47 *Salmonella,* the long helical flagellar filament propeller that extends from the cell
48 surface is connected to a flexible hook attached to a basal body spanning the cell
49 envelope. These flagellar substructures are assembled in a strict order, with the
50 basal body being constructed first, followed by the hook and then the filament [1, 2].
51 The filament comprises thousands of copies of the major filament subunit, FliC
52 (flagellin), together with three minor filament-class subunits: eleven copies each of
53 FlgK and FlgL form a junction connecting the semi-rigid filament to the hook, and five
54 FliD subunits assemble at the distal tip of the nascent flagellum to form a cap that
55 facilitates folding and incorporation of flagellin into the growing filament [3].
56
57 Export of the filament subunits is facilitated by the cytoplasmic chaperones FlgN, FliT
58 and FliS, which bind the C-terminal domains of their cognate structural subunits
59 (FlgN binds FlgK and FlgL, FliT binds FliD, and FliS binds FliC) [4-6]. The
60 chaperones then pilot their cognate subunits to the specialized flagellar Type III
61 secretion system (fT3SS) machinery at the base of each flagellum [7-11].
62 Chaperone-subunit complexes initially dock at the FliI component of the flagellar
63 export ATPase, which is evolutionarily related to the F1-ATPase [12]. Chaperoned
64 subunits are then thought to interact with the integral membrane export gate
65 component FlhA, where chaperones are released and the subunit cargo is unfolded
66 for translocation across the inner membrane, *via* the FlhAB-FliPQR export gate, into
67 a narrow central channel in the growing flagellum [9-13]. Once released from their
68 cognate subunit cargo, the unladen chaperones FlgN and FliT - but not the flagellin
69 chaperone, FliS - are recruited by the FliJ stalk component of the ATPase, which

transfers them to newly synthesised cognate cargo to create a local cycle of chaperone-subunit binding at the membrane fT3SS [8]. This is thought to promote export of the minor filament subunits that form the hook-filament junction and the filament cap, which are required for initiation of filament assembly [14].

Export of flagellar subunit cargo across the membrane is powered by the pmf and the flagellar ATPase complex [15, 16]. Specifically, the ATPase is thought to facilitate unfolding of subunit cargo [17]. In addition, analogous to F- and V-type ATPases, ATP hydrolysis is proposed to drive rotation of the ATPase stalk, FliJ, which interacts with the nonameric export gate component, FlhA, converting the gate into a highly efficient proton-protein antiporter that utilises the $\Delta\Psi$ electric component of the pmf [18]. The FliJ-FlhA interaction is essential for export gate activation, and disruption of this interaction renders the export gate inactive and attenuates protein export [18].

What is currently unclear is how FliJ activation of the export gate is regulated in the absence of subunit cargo to prevent constitutive proton influx and wasteful dissipation of the pmf. One way in which export gate activation could be regulated is by sequestration of FliJ by other binding partners, specifically the export chaperones FlgN and FliT. A role for chaperones in the regulation of T3SS activity is supported by the finding that the *Psuedomonas* virulence T3SS chaperone PcrG binds the FliJ homologue, PscO, and that loss of this interaction results in upregulation of effector secretion and renders the T3SS more resistant to pmf collapse [19]. These observations suggest that the chaperone-FliJ interaction is central to the regulation of T3SS activity, however, the mechanistic basis of this regulation remains obscure.

95

96 Here, we identify point mutant variants of the chaperones FlgN and FliT that are
97 specifically defective for binding to the FliJ ATPase stalk yet retain the ability to bind
98 cognate subunits and the FlhA component of the fT3SS export gate. We show *in*
99 *vitro* that the FlgN and FliT chaperones compete with FlhA for binding to FliJ, and
100 that chaperone sequestration of FliJ *in vivo* blocks the activating interaction between
101 FliJ and the export gate. This suggests a mechanism whereby binding of FliJ by
102 unladen chaperones acts as a signal to the export machinery that subunit cargo is
103 unavailable and, accordingly, export activity is limited to prevent wasteful dissipation
104 of the pmf. This model is supported by ribosome profiling data, which show that the
105 cytoplasmic ratios of cognate subunits to chaperones are low for FlgN and FliT,
106 relative to the ratio of flagellin to its chaperone, FliS, suggesting that levels of
107 unladen FlgN and FliT would be a sensitive proxy measure of intracellular flagellar
108 subunit levels. Our data indicate a mechanism by which chaperones modulate the
109 FliJ-FlhA interaction to regulate energy use by the T3SS in response to subunit
110 availability.

111

112 **Results**

113 ***Isolation of chaperone variants that are specifically defective for FliJ binding***

114 To investigate the function of chaperone binding to the ATPase stalk, FliJ, we sought
115 to identify variants of the FlgN and FliT chaperones that did not bind FliJ yet could
116 interact with cognate subunits and the FlhA component of the fT3SS export gate. To
117 do this, we first constructed mutant alleles of *flgN* encoding variants with three-
118 residue deletions in the FlgN α3 helix (residues 70-102), which contains the
119 overlapping binding sites for cognate subunits and FliJ (Fig. 1; *SI Appendix*, Fig. S1)

120 [8]. Screening of the FlgN deletion variants using affinity chromatography pull-down
121 assays with GST- FlgK subunit or GST-FliJ identified a single deletion variant,
122 FlgNΔ76-78, that could bind its cognate subunit but not the ATPase stalk (Fig. 1*B*).
123 Protein sequence comparisons revealed FlgN W_{78} to be highly conserved and
124 replacement of this residue with alanine (FlgN-W_{78}A) severely reduced FlgN binding
125 to FliJ but did not affect binding to FlgK subunit (Fig. 1*C*; FlgNΔ90-100, which binds
126 neither cognate subunit nor FliJ, and wild type FlgN were included as negative and
127 positive controls, respectively) [8]. Affinity chromatography pull-down assays
128 confirmed that FlgNΔ76-78 and FlgN-W_{78}A could still bind the cytoplasmic domain of
129 the export gate component FlhA (GST-$FlhA_C$; Fig. 1*C*; interactions between FlgN
130 variants and their binding partners are summarised in SI Appendix Table 3).
131
132 Having identified residues in the FlgN α3 helix that, when mutated, could decouple
133 chaperone binding of cognate subunits and FliJ, we targeted conserved residues in
134 the equivalent α3 helix of FliT for site directed mutagenesis to alanine (Fig. 1*D*; *SI*
135 *Appendix*, Fig. S1). To facilitate screening for FliJ binding, mutations were introduced
136 into a *fliT* allele encoding a truncated variant, $FliT_{94}$, which lacks the α4 helix and
137 shows enhanced binding to FliJ *in vitro* [20]. Affinity chromatography pull-down
138 assays identified five $FliT_{94}$ variants (I_{68}A, L_{72}A, N_{74}A, E_{75}A and L_{78}A) that showed
139 severely reduced binding to GST-FliJ (Fig. 1*E*). Three of these FliJ non-binders -
140 $FliT_{94}$-I_{68}A, $FliT_{94}$-L_{72}A and $FliT_{94}$-N_{74}A - had previously been shown to bind cognate
141 subunit FliD [20]. For this reason, and after assessing the expression and stability of
142 these three $FliT_{94}$ variants in *Salmonella* (not shown), we chose to further investigate
143 the function of truncated $FliT_{94}$-L_{72}A and full-length FliT-L_{72}A.
144

145 Binding of FliT-L_{72}A and truncated $FliT_{94}$-L_{72}A to cognate subunit FliD was confirmed
146 using pull-down assays (GST-FliD; *SI Appendix*, Fig. S2). To assess binding to the
147 export gate component FlhA, pull-down assays were carried out using GST-$FlhA_C$
148 that had been incubated with cell lysates containing FliD cognate subunit, which is
149 required for high affinity binding of FliT to FlhA, and either wild type FliT or full-length
150 FliT-L_{72}A (Fig. 1*F*) [9]. The FliT-Y_{106}A variant, which cannot bind FlhA, was included
151 as a negative control (Fig. 1*F*) [11]. Data from the pull-down assays indicated that,
152 when bound to cognate subunit FliD, the FliT-L_{72}A variant can bind the FlhA export
153 gate (Fig. 1*F*; interactions between FliT variants and their binding partners are
154 summarised in SI Appendix, Table 4).
155

156 ***Attenuation of cell motility and cognate subunit export by specific disruption***
157 ***of the chaperone-FliJ interaction***

158 Having identified chaperone variants (FlgNΔ76-78, FlgN-W_{78}A, FliT-L_{72}A) that were
159 specifically defective for FliJ binding yet retained the ability to bind cognate subunits
160 and the fT3SS export gate, we went on to investigate the importance of the
161 chaperone-FliJ interaction for cell motility and subunit export. To enable expression
162 of chaperones at physiological levels, *Salmonella* strains were engineered to carry
163 variant chaperone genes (*flgNΔ76-78*, *flgN-W_{78}A* or *fliT-L_{72}A*) at the natural genetic
164 loci, replacing the wild type chaperone genes. As negative controls, isogenic
165 *Salmonella* strains in which the chaperone genes were either deleted (Δ*flgN* or Δ*fliT*)
166 or replaced with variant genes encoding export defective chaperones unable to bind
167 either cognate subunit (*flgNΔ90-100*) or the FlhA export gate (*fliT-Y_{106}A*) were also
168 constructed. These strains were assessed for swimming and swarming motility, and
169 for subunit export efficiency relative to wild type *Salmonella* (Fig. 2).

170

171 Cell populations producing the FlgNΔ76-78 or FlgN-W_{78}A variants, which cannot
172 bind FliJ, showed slightly decreased swimming (70-90%) and swarming (75-90%)
173 motility relative to wild type *Salmonella*, though their motility was significantly better
174 than that of the *flgN* null strain or cells producing FlgNΔ90-100, which binds neither
175 cognate subunits nor FliJ (Fig. 2*A* and *SI Appendix*, Fig. S2). Secretion of cognate
176 subunit FlgK was also reduced to *c.*50% of wild type in cells producing either
177 FlgNΔ76-78 or FlgN-W_{78}A, and this was accompanied by a concomitant increase in
178 soluble extracellular FliC (to 140-150% of wild type), suggesting that assembly of the
179 FlgKL hook-filament junction was impaired, causing inefficient initiation of filament
180 assembly and increased release of unpolymerized FliC into culture supernatants
181 (Fig. 2*B*) [4]. As expected, this secretion defect was more severe in the *flgN* null
182 strain and in cells producing FlgNΔ90-100 (Fig. 2*B*).
183

184 Analysis of motility and export phenotypes associated with the FliT chaperone is
185 complicated by the additional function of FliT as a negative regulator of the flagellar
186 master transcriptional activator $FlhD_4C_2$ [21-23]. Cells lacking FliT show increased
187 cellular levels of $FlhD_4C_2$, and a concomitant increase in flagellar gene expression
188 that partially alleviates the motility and export defects typically associated with loss of
189 chaperone activity [4]. The increased flagellar gene expression in the *fliT* null is
190 reflected by an increase in the cellular level of non-cognate subunit FlgK, which was
191 observed to be 1.4-fold higher than in wild type (*SI Appendix*, Fig. S3). Similarly, the
192 level of FlgK was 1.4-fold higher in the strain producing the export defective FliT-
193 Y_{106}A (*SI Appendix*, Fig. S3), indicating increased flagellar gene expression that may
194 be caused by sequestration of FliT-Y_{106}A by cytosolic FliD, which would prevent FliT-

195 $Y_{106}A$ binding to FlhC and targeting it for degradation [21-23]. However, cellular
196 levels of FlgK in cells producing FliT-$L_{72}A$ were similar to wild type, suggesting that
197 while FliT-$L_{72}A$ cannot bind FliJ, it retains the ability to bind FlhC and thus regulate
198 flagellar gene expression (*SI Appendix*, Fig. S3).
199
200 Cells producing FliT-$L_{72}A$ displayed wild type swimming motility but showed a
201 significant defect in population swarming motility relative to wild type *Salmonella*
202 (*c.*50% of wild type; Fig. 2A). Moreover, export of cognate subunit FliD was reduced
203 to *c.*50% of wild type in the FliT-$L_{72}A$ strain. These data suggest that the FliT-FliJ
204 interaction may be required for export of sufficient FliD to promote the increased
205 flagellation required for swarming [24, 25]. Cells producing FliT-$Y_{106}A$, which cannot
206 bind FlhA, showed only a slight defect in swimming and swarming motility, while the
207 *fliT* null strain displayed a marginal reduction in swimming to *c.*80% of wild type, yet
208 an increase in swarming motility (to *c.*110% of wild type; Fig. 2B). Both the *fliT* null
209 and FliT-$Y_{106}A$ strain showed a significant reduction in FliD export, to 50-60% of wild
210 type, accompanied by concomitant release of unpolymerized FliC to culture
211 supernatants (to 110% of wild type; Fig. 2B). The confounding influence of increased
212 flagellar gene expression in these strains, however, makes it difficult to interpret the
213 motility and export phenotypes of the *fliT* null and FliT-$Y_{106}A$ controls, particularly as
214 overexpression of *flhDC* is known to overcome motility defects associated with
215 chaperone loss [26, 27].
216
217 Notwithstanding the difficulties in interpreting the motility and flagellar export
218 phenotypes associated with loss or mutation of *fliT*, the data for FlgNΔ76-78, FlgN-
219 $W_{78}A$ and FliT-$L_{72}A$ indicate that specific loss of chaperone interactions with FliJ,

220 which would break the local chaperone cycle at the fT3SS, result in attenuation of
221 cognate subunit export and cell motility. That motility and subunit export are only
222 partially attenuated by disruption of the chaperone-FliJ interaction indicates that the
223 variant chaperones are still able to pilot cognate subunits to the fT3SS machinery to
224 promote export. The data suggest that chaperone binding by FliJ increases the
225 efficiency of, but is not essential for, cognate subunit export (Fig. 2). This raises a
226 question as to whether the chaperone-FliJ interaction might have an additional
227 function related to the primary role of FliJ in activating the export machinery to
228 couple efficient use of the pmf to protein export [18].
229
230 ***Unladen chaperones disrupt the FliJ-FlhA$_C$ interaction***
231 The identification and characterisation of FlgN and FliT chaperone variants that
232 retained their subunit piloting function but were specifically unable to bind the FliJ
233 ATPase stalk opened up the possibility of further investigations into whether
234 chaperones might regulate FliJ activation of the fT3SS. To test whether unladen
235 chaperones could bind FliJ and block the FliJ interaction with the FlhA export gate,
236 we developed an *in vitro* competition assay in which FlhA$_C$ binding to cobalt bead-
237 immobilized (His)$_6$-FliJ was assessed in the presence of chaperone variants that
238 could interact with FliJ but not FlhA$_C$ (FliT$_{94}$ or FlgN-Y$_{122}$A) or were defective in
239 binding both FliJ and FlhA$_C$ (FliT$_{94}$-L$_{72}$A or FlgN-Y$_{122}$AΔ76-78; Fig. 3*A*). The
240 chaperone variants were engineered to be defective for binding to FlhA$_C$ (by
241 introduction of the FliT$_{94}$ or FlgN-Y$_{122}$A mutations) to prevent chaperone-FlhA$_C$
242 interactions and thus allow specific analysis of the effect of chaperone-FliJ binding
243 on the FlhA$_C$-FliJ interaction. This assay, therefore, specifically interrogates the

244 effect that chaperones have on the FliJ-FlhAc interaction in the absence of
245 interfering chaperone-$FlhA_C$ interactions (Fig.3A; [8-11]).
246
247 As anticipated, we found that $FlhA_C$ could bind $(His)_6$-FliJ in the presence of
248 chaperone variants that could not bind FliJ (Fig. 3*B*). However, when assays were
249 performed with chaperones that could bind FliJ, the amount of $FlhA_C$ pulled down by
250 FliJ was severely reduced (Fig. 3*B*). These data show that FlgN and FliT can
251 compete with $FlhA_C$ for binding to FliJ*, i.e.* unladen chaperones bound to FliJ prevent
252 the FliJ-$FlhA_C$ interaction – an interaction known to be essential for activation of the
253 export gate to efficiently couple pmf use to protein export [18].
254
255 ***Regulation of fT3SS export gate activation in vivo by chaperone sequestration***
256 ***of the FliJ ATPase stalk***
257 The *in vitro* competition assay established that the FlgN and FliT chaperones could
258 block FliJ binding to $FlhA_C$, but did not show whether activation of the $FlhA_C$ export
259 gate was prevented. To investigate this, an *in vivo* competition assay was developed
260 in which the effect of FlgN-FliJ binding on $FlhA_C$ export activity was tested under
261 conditions where the availability of cognate subunits for FlgN was limited.
262 Specifically, FlgN variants that could bind FliJ but not $FlhA_C$ (FlgN-Y_{122}A) or were
263 defective in binding both FliJ and $FlhA_C$ (FlgN-Y_{122}AΔ76-78) were expressed *in trans*
264 in a Δ*flgE* strain, in which flagellar assembly does not progress beyond completion of
265 the rod, and the FlgN cognate subunits, FlgK and FlgL, are produced at very low
266 levels (*SI Appendix*, Fig. S4) [28-30]. As cognate subunit levels are low in the Δ*flgE*
267 strain, we hypothesised that *in trans* overexpression of *flgN-Y_{122}A* would produce an
268 excess of unladen FlgN-Y_{122}A that would bind FliJ and disrupt the FliJ-$FlhA_C$

interaction, preventing activation of the flagellar export gate and inhibiting subunit export. Conversely, we hypothesised that similar overproduction of the FlgN-$Y_{122}A\Delta$76-78 variant, which cannot bind FliJ, would not disrupt the FliJ-$FlhA_C$ interaction, and would permit FliJ-dependent activation of the export gate and efficient subunit export.

Assays of subunit export in a strain producing FlgN-$Y_{122}A$, which binds FliJ, demonstrated a *c.*75% reduction in export of the FlgD subunit compared to a strain producing FlgN-$Y_{122}A\Delta$76-78, which cannot bind FliJ (Fig *3C*). The data indicate that when unladen chaperones are present in the cell (as would occur when their cognate subunit levels are low) non-cognate subunit export is attenuated by the unladen chaperones specifically binding to FliJ, preventing export gate activation.

Taken together, the data from the *in vitro* and *in vivo* competitive binding assays indicate that unladen chaperones block the FliJ-FlhA interaction and prevent FliJ-dependent activation of the flagellar export machinery. How, then, are unladen chaperones released from FliJ, enabling export activity to be restored once cognate subunit levels return to normal? Evans and colleagues previously demonstrated that cognate subunits can capture unladen chaperones from FliJ, which would effectively free FliJ to bind the FlhA export gate and restore subunit export [8]. This provides an elegant mechanism whereby an unladen chaperone remains docked at FliJ, inhibiting pmf-driven export, until a cognate subunit is available to capture the chaperone from FliJ, allowing export activity to resume.

293 ***Ribosome profiling reveals low cytoplasmic ratios of minor filament subunits***
294 ***to their cognate chaperones, FlgN and FliT***
295 Our accumulating data suggested that, in addition to piloting subunit cargo to the
296 fT3SS, the FlgN and FliT chaperones might be conditional regulators of fT3SS
297 activity, which sense and respond to the availability of subunit cargo. To function
298 effectively in the cell, this mechanism - in which unladen chaperones are a proxy
299 measure for subunit availability - would require cytoplasmic ratios of FlgN/FliT to
300 their cognate subunits to be low. To obtain an indication of the cytoplasmic levels of
301 chaperones and their cognate subunits, we used RNA sequencing (RNA-Seq) and
302 ribosome profiling (Ribo-Seq) to assess the *Salmonella* global transcript abundance
303 and translatome, respectively, at late-log growth phase when flagellar gene
304 expression is at its peak [31-34]. Analysis of these data confirmed that flagellar
305 mRNAs are amongst the most abundant and highly translated in *Salmonella* (Fig.
306 4*A*). The ribosome profiling data indicated that the ratio of FlgN to its cognate
307 subunits (FlgK and FlgL) was 1:3, and the ratio of FliT to its cognate subunit FliD
308 was 1:4. These chaperone-subunit ratios are low when compared to the 1:43 ratio of
309 FliS chaperone to its cognate subunit FliC (Fig. 4*B*), suggesting that the presence of
310 unbound FlgN and FliT in the cell would provide a sensitive proxy measure of
311 cytoplasmic flagellar subunit levels. Taken together with our other findings, these
312 data strengthen the view that, when unladen, the FlgN and FliT chaperones couple
313 subunit availability to pmf-driven export by modulating FliJ-dependent activation of
314 the $FlhA_C$ export gate.
315
316
317

318 **Discussion**

319 The synthesis and operation of bacterial flagella is energetically expensive, using an
320 estimated 2% of the cell's energy, and numerous regulatory mechanisms have
321 evolved to increase efficiency of flagella biogenesis and function. Here, we have
322 uncovered the mechanism by which fT3SS chaperones couple the availability of
323 subunit cargo to the energy efficiency of flagellar export. By identifying point mutant
324 variants of the FlgN and FliT chaperones that were specifically unable to bind the
325 FliJ stalk component of the fT3SS ATPase, we showed that the chaperone-FliJ
326 interaction prevents activation of the FlhA export gate component when subunit
327 availability is low, reducing wasteful dissipation of the pmf by the fT3SS machinery.
328

329 ***Mutational analysis of the FlgN and FliT chaperones reveals key residues***
330 ***specifically required for binding to the FliJ ATPase stalk***

331 Our mutational analysis identified FlgN chaperone variants, FlgN $W_{78}A$ and
332 FlgNΔ76-78, which were defective in binding to FliJ but could still pilot their cognate
333 subunits FlgK and FlgL to dock at the export gate component $FlhA_C$ (Fig.1). Motility
334 of strains producing FlgN $W_{78}A$ or FlgNΔ76-78 was marginally reduced compared to
335 wild type, as was export of FlgK and FlgL, indicating that loss of the FlgN-FliJ
336 interaction reduced the efficiency of, but did not abolish, cognate subunit export (Fig.
337 2).
338

339 Mutational analysis of the FliT chaperone showed that several highly conserved,
340 surface exposed residues on the helix required for cognate subunit binding were also
341 critical for binding to FliJ (Fig.1C). Replacement of FliT leucine-72 with alanine was

342 found to disrupt binding to FliJ, but did not affect FliT chaperone interactions with
343 FliD cognate subunit or $FlhA_C$ (Fig. 1). Cells producing FliT $L_{72}A$ did not display a
344 swimming motility defect compared to wild type *Salmonella* (Fig. 2C). However, a
345 marginal export defect was observed for cognate subunit FliD (Fig. 2D). Cells
346 producing FliT $L_{72}A$ displayed reduced population swarming, indicating that the FliT-
347 FliJ interaction may be required for the hyperflagellation associated with this form of
348 surface motility.

349 ***Unladen chaperones modulate the interaction of the FliJ ATPase stalk with the***
350 ***cytoplasmic domain of the FlhA export gate***

351 A previous study showed that FliJ appeared to enhance the binding of a FliT/FliD
352 complex to $FlhA_C$ [9]. Using affinity chromatography of resin-bound GST-$FlhA_C$ with
353 a complex of FliT-FliD it was observed that when assays contained FliJ, binding of
354 FliT-FliD to GST-$FlhA_C$ appeared to increase [9]. The addition of excess unladen FliT
355 chaperone to the pull-down assay reversed the FliJ-dependent binding enhancement
356 [9]. As other studies have shown that unladen FliT chaperone does not bind $FlhA_C$,
357 we propose that FliT would block the FliJ-$FlhA_C$ interaction (Figs. 4 and 5),
358 preventing the FliJ-dependent enhancement of FliT/FliD binding to $FlhA_C$, as
359 observed by Bange and colleagues [9, 11, 35].
360

361 We have previously shown that FliJ-bound chaperones are efficiently captured by
362 their cognate subunits to establish a local chaperone cycle at the membrane export
363 machinery, which increases the efficiency of subunit export [8]. In this mechanism,
364 the absence of cognate subunits would disrupt the chaperone cycle, resulting in
365 unladen chaperones remaining docked at FliJ. The data presented here show that

366 this chaperone-FliJ interaction would block FliJ-dependent activation of the flagellar
367 export gate, preventing unnecessary activation of the export gate in the absence of
368 subunits. In the situation where cellular levels of cognate subunit increase,
369 chaperones would be captured from FliJ, restoring FliJ-dependent activation of the
370 export gate and subsequent subunit export (Fig. 6).
371
372 It is well established that an interaction between FliJ and the FlhA export gate protein
373 is required for efficient ΔΨ-driven protein export [18]. The FliH and FliI components
374 of the ATPase support the FliJ-FlhA interaction, and hydrolysis of ATP by the
375 ATPase complex is proposed to drive rotation of FliJ, allowing it to contact
376 sequentially all nine monomers of the FlhA nonameric ring, converting the export
377 machinery into a highly efficient proton-protein antiporter [12,15,16,18]. The fT3SS
378 ATPase components share many features of the F_1 ATP synthase: FliI and FliJ
379 share considerable structural similarity to the α/β- and γ-subunits, respectively, and
380 FliH shares considerable amino acid sequence similarity to the b and δ subunits [36].
381 Furthermore, analogous to the F_0 ATP synthase component, the flagellar export
382 machinery harnesses the power of the pmf [12, 37]. Multiple mechanisms have been
383 identified that regulate both ATPase activity and pmf use by the F_1F_0-ATP synthase,
384 including proteins that inhibit efficient coupling between the F_1 and F_0 components
385 [37-39]. Our data demonstrate that unladen export chaperones disrupt FliJ-
386 dependent activation of the flagellar export gate, which would prevent wasteful pmf
387 use in the absence of cognate subunits, by effectively preventing a FliJ-FlhA
388 interaction until the chaperone is captured from FliJ by a cognate subunit, relieving
389 the inactive state.
390

391 ***A mechanism coupling export gate activation to availability of subunits for***
392 ***export***
393 Our data support a model whereby, when subunits are at low levels in the cell,
394 unladen FlgN and FliT bind to FliJ, preventing the FliJ-FlhA interaction and
395 subsequent activation of the export gate. Ribosome profiling revealed the amounts of
396 chaperone and cognate subunit(s) produced by the cell and while all three flagellar
397 chaperones are produced at similar levels (Fig. 6), the intracellular ratio of
398 chaperone to subunit is low for the FlgN and FliT chaperones (1:3 and 1:4,
399 respectively), compared to the ratio of FliS chaperone to flagellin (1:43), which is
400 produced and exported at far higher levels than FlgK and FlgL [8]. As a result, the
401 presence of unladen FlgN and FliT would serve as a sensitive proxy measure for
402 changes in the availability of newly synthesised flagellar subunits in the cell, as these
403 chaperones are more likely to be free, compared to the FliS chaperone, when
404 subunit levels drop. This may in part explain why FliS has not evolved to bind FliJ.
405
406 Whether such a mechanism of chaperone mediated coupling of subunit availability to
407 export gate activation occurs in the related vT3SS is not clear. However, a subset of
408 export chaperones, specifically for the virulence needle translocon and tip subunits,
409 bind to vT3SS FliJ homologues [19, 40, 41, 46]. Notably, an export chaperone
410 (PcrG) in *Pseudomonas aeruginosa* binds to the FliJ homologue (PscO) and
411 modulates pmf use by the vT3SS, although the mechanistic basis for this was
412 unclear [19]. Independent to PscO (FliJ) binding, and in the absence of cognate
413 subunit, PcrG can regulate effector secretion through interactions with the FlhA
414 homologue, PcrD, preventing effectors accessing the export machinery [19]. These
415 findings indicate that interactions between a subset of export chaperones and FliJ

416 homologues may be conserved among vT3SSs. Whether these binding events also
417 serve to regulate export gate activation with respect to subunit availability is yet to be
418 determined.
419
420 Chaperone modulation of fT3SS activity may be important when *Salmonella*
421 encounters environmental conditions in which flagellar gene expression is down-
422 regulated, including during the early stages of host infection [42-45]. Our data
423 support a model for a local chaperone cycle at the T3SS machinery that (i) facilitates
424 efficient docking and export of cognate subunit cargo when subunit/effector
425 availability is high, and (ii) prevents constitutive proton influx and wasteful dissipation
426 of the pmf when subunit cargo availability is low (Fig. 6).
427
428 **Materials and Methods**
429 **Bacterial strains, plasmids and growth conditions**
430 Wild type *Salmonella enterica* serovar Typhimurium (*S. typhimurium*) SJW1103 is
431 motile [48]. The Δ*fliT*::K_m^R mutant in which the *fliT* gene was replaced by a
432 kanamycin resistance cassette was constructed using the λ Red recombinase
433 system [49]. Strains containing chromosomally encoded FliT or FlgN variants were
434 constructed by *aph*-I-SceI Kanamycin resistance cassette replacement using
435 pWRG730 [49]. Bacteria were cultured at 30–37°C in Luria-Bertani (LB) broth
436 containing, where appropriate, ampicillin (100 μg/ml) or chloramphenicol (20 μg/ml)
437 and collected by centrifugation (6,000*g* for 10 min). Recombinant proteins were
438 expressed in *Salmonella* from the isopropyl β-D-thiogalactoside-inducible (IPTG)-
439 inducible plasmid pTrc99a [50].
440

441 Recombinant proteins for purification were expressed in *E.coli* C41 [51] from (IPTG)-
442 inducible pACT7 [52] or pGEX-4T3 [53]. To construct recombinant plasmids
443 encoding wild type or derivative genes, *Salmonella* genes were amplified from
444 chromosomal DNA by PCR or overlap-extension PCR using Q5 High-Fidelity DNA
445 polymerase. PCR products were inserted BamHI/XhoI into pGEX-4T3 or
446 NdeI/BamHI into pACT7 and pTrc99a. Inserts were verified by DNA sequencing
447 (Department of Biochemistry, University of Cambridge). A full list and description of
448 strains and plasmids used in this study can be found in *SI Appendix*, Tables S1 and
449 S2.
450
451 **Affinity chromatography co-purification assays**
452 Co-purification of proteins expressed in *E.coli* C41 was performed with glutathione-
453 sepharose 4B. Cells were resuspended in buffer A (50 mM sodium phosphate
454 pH7.4, 150 mM NaCl, 1mM β–mercaptoethanol) and mechanically lysed with a
455 Constant Systems cell disruptor at 30,000 kPa. Cleared lysates containing GST-
456 tagged proteins were incubated with affinity resin for 1 hour. After extensive washing
457 with buffer A, cell lysates containing overexpressed untagged prey proteins were
458 then incubated with the resin pre-bound GST-bait. Resins were washed extensively
459 with buffer A and proteins eluted by boiling in SDS-PAGE loading buffer. Proteins
460 were separated by SDS-PAGE and immunoblotted.
461
462 **Flagellar subunit export assay**
463 *Salmonella* strains were cultured at 37 °C in LB broth containing ampicillin and 100
464 μM IPTG to mid-log phase (A_{600} 0.6-0.8). Cells were centrifuged (6000*g*, 5 min),
465 resuspended in fresh media and grown for a further 60 min at 37 °C. Cells were

466 pelleted by centrifugation (16,000*g*, 5 min) and the supernatant passed through a 0.2
467 µm nitrocellulose filter. Supernatant proteins were precipitated with 10%
468 trichloroacetic acid (TCA) and 1% Triton-X100 on ice for 1 hour, pelleted by
469 centrifugation (16,000*g*, 10 min), washed with ice-cold acetone and resuspended in
470 SDS-PAGE loading buffer (volumes calibrated according to cell densities). Fractions
471 were analysed by immunoblotting.
472
473 **Motility assays**
474 For swimming motility, *Salmonella* strains were grown in LB broth to A_{600} 1. Two
475 microliters of culture were inoculated into soft tryptone agar (0.25% agar, 10 g/L
476 tryptone, 5g/L NaCl). Plates were incubated at 37 °C for between 4 and 6 hours. For
477 swarming motility, one microliter of overnight cultures grown in LB broth was
478 inoculated onto dried tryptone agar plates (0.6% agar, 10g/L tryptone, 5g/L NaCl)
479 supplemented with 0.3% glucose and incubated at 30 °C for 16 hours.
480
481 **Chaperone-FliJ *in vitro* competition assay**
482 Recombinant proteins were expressed in *E.coli* C41 and cells were mechanically
483 lysed as described for the co-purification assays. Cleared lysates containing His-
484 tagged FliJ were incubated with cobalt affinity resin for 1 hour. After extensive
485 washing, cell lysates containing overexpressed untagged $FlhA_C$ was added to each
486 resin fraction and an equal volume of wild type $FliT_{94}$, $FliT_{94}$ $L_{72}A$, wild type FlgN or
487 FlgN $W_{78}A$ was added. Proteins were incubated for 1 hour, the resin was washed
488 extensively with buffer A and proteins were eluted by boiling in SDS-PAGE loading
489 buffer. Proteins were separated by SDS-PAGE and immunoblotted.
490

491 **FlgN-FliJ *in vivo* competition assay**

492 *Salmonella flgE* null strains carrying either pTrc99a encoding *flgN*-$Y_{122}A\Delta$76-78 or
493 *flgN*-$Y_{122}A$ were grown in LB broth containing ampicillin and inducing agent (50 μM
494 IPTG) to A_{600} 1.0. Cells were centrifuged (6000*g*, 5 min) and resuspended in fresh
495 media and grown for a further 60 min at 37°C. Cells were pelleted by centrifugation
496 (16,000*g*, 5 min) and the supernatant passed through a 0.22 μm nitrocellulose filter
497 (Sartorius). Proteins were precipitated with 10% trichloroacetic acid (TCA) and 1%
498 Triton- X100 on ice for 1 hour, pelleted by centrifugation (16,000*g*, 10 min, 4°C),
499 washed with ice-cold acetone and resuspended in SDS-PAGE loading buffer
500 (volumes calibrated according to cell densities). Fractions were analysed by
501 immunoblotting.

502

503 **Ribosome profiling and RNA-Seq**

504 Libraries were prepared essentially as described previously [54, 55] with the
505 following modifications: Cells were grown in LB at 37°C with 180 RPM shaking to
506 A_{600} 1.0. Chloramphenicol was added to the culture to a final concentration of 1500
507 μg/ml, followed by rapid cooling of the culture and harvesting of cells by
508 centrifugation (6,000 g, 1 min, 4°C). The cell pellet was quickly resuspended in 1 ml
509 ice cold bacterial profiling buffer (20 mM Tris-Cl pH 7.5, 140 mM KCl, 5 mM $MgCl_2$,
510 1500 μg/ml chloramphenicol, 0.5 mM dithiothreitol (DTT), 0.5% NP40, 1% Triton X-
511 100, 2.5% Sucrose) and flash-frozen for cryo-grinding in liquid nitrogen. The frozen
512 powder was thawed and clarified by centrifugation (13,000 g, 2 mins, 4°C) followed
513 by adjustment of $A_{254\ nm}$10. Lysates were either snap frozen in liquid nitrogen for
514 storage at -80°C or nuclease treated with RNase 1 (700U, Ambion) followed by
515 ribosomal RNA depletion using a bacterial ribozero kit (Illumina) prior to library

516 preparation for ribosome profiling. For parallel RNA-Seq, total RNA was extracted
517 from corresponding lysates followed ribosomal RNA depletion using the bacterial
518 ribozero kit (Illumina) prior to library preparation. For Ribosome profiling, rRNA was
519 further depleted with duplex-specific nuclease as described previously [54].
520 Ribosome profiling and RNA-Seq libraries were pooled and sequenced using the
521 NextSeq® 500/550 platform and data were trimmed and mapped to the
522 transcriptome assembly of *Salmonella enterica* subsp. *enterica* serovar Typhimurium
523 strain ST4/74 (GenBank accession CP002487.1). Paired ribosome profiling and
524 RNA-Seq analysis was performed with riboSeqR as previously described [55, 56].
525

526 **Quantification and statistical analysis**

527 Experiments were performed at least three times. Immunoblot data were quantified
528 using Image Studio Lite. The unpaired two-tailed Student's *t*-test was used to
529 determine *p*-values, and significance was defined as $*p < 0.05$. Data are represented
530 as mean ± standard error of the mean (SEM), unless otherwise specified and
531 reported as biological replicates.
532

533 **Acknowledgements**

534 We thank Colin Hughes and Lewis Evans for useful discussions, and Sangita Ahmed
535 for technical assistance. This work was funded by grants from the Biotechnology and
536 Biological Sciences Research Council (BB/M007197/1) to G.M.F, Medical Research
537 Council [MR/R021821/1] to B.Y-W.C., and a University of Cambridge John Lucas
538 Walker Studentship to O.J.B.
539
540

541 **Footnotes**

542 The authors declare no conflict of interest.

543

544 **Author contributions**

545 **Owain J. Bryant**: Conceptualization, Data curation, Investigation, Formal analysis,
546 Methodology, Visualisation, Writing – original draft, Writing – review & editing. **Betty**
547 **Y-W Chung**: Data curation, Formal analysis, Funding acquisition, Methodology,
548 Investigation, Visualisation, Software, Writing – original draft, Writing – review &
549 editing. **Gillian M. Fraser**: Conceptualization, Data curation, Formal analysis,
550 Funding acquisition, Investigation, Methodology, Project administration, Resources,
551 Supervision, Visualisation, Writing – original draft, Writing – review & editing.

552

553 **References**

554 1. Evans, L. D. B., Hughes, C. & Fraser, G. M. (2014). Building a flagellum
555 outside the bacterial cell. *Trends Microbiol.* 22, 566-572.
556 2. Evans, L. D. B., Hughes, C. & Fraser, G. M. (2014). Building a flagellum in
557 biological outer space. *Microb. Cell.* 1, 64-66
558 3. Yonekura, K., Maki, S., Morgan, D. G., DeRosier, D. J., Vonderviszt, F.,
559 Imada, K. & Namba, K. (2000). The bacterial flagellar cap as the rotary
560 promoter of flagellin self-assembly. *Science* 290, 2148-2152.
561 4. JBennett, J. C., Thomas, J., Fraser, G. M. & Hughes, C. (2001). Substrate
562 complexes and domain organization of the *Salmonella* flagellar export
563 chaperones FlgN and FliT. *Mol. Microbiol*. 39, 781–791
564 5. Fraser, G.M., Bennett, J.C. & Hughes, C. (1999). Substrate-specific binding of
565 hook-associated proteins by FlgN and FliT, putative chaperones for flagellum

566 assembly. *Mol. Microbiol.* 32, 569–580
567 6. Auvray, F., Thomas, J., Fraser, G. M. & Hughes, C. (2001). Flagellin
568 polymerisation control by a cytosolic export chaperone. *J. Mol. Biol.* 308:221–
569 229
570 7. Thomas, J., Stafford, G. P. & Hughes, C. (2004). Docking of cytosolic
571 chaperone-substrate complexes at the membrane ATPase during flagellar type
572 III protein export. *Proc. Natl. Acad. Sci USA* 101, 3945-3950
573 8. Evans, L. D. B., Stafford, G. P., Ahmed, S., Fraser, G. M. & Hughes, C. (2006).
574 An escort mechanism for cycling of export chaperones during flagellum
575 assembly. *Proc. Natl. Acad. Sci. USA* 103, 17474–9
576 9. Bange, G., Kümmerer, N., Engel, C., Bozkurt, G., Wild, K. & Sinning, I. (2010).
577 FlhA provides the adaptor for coordinated delivery of late flagella building
578 blocks to the type III secretion system. *Proc. Natl. Acad. Sci. USA* 107, 11295–
579 11300.
580 10. Minamino, T., Kinoshita, M., Hara, N., Takeuchi, S., Hida, A., Koya, S.,
581 Glenwrright, H., Imada, K., Aldridge, P. D. & Namba, K. (2012). Interaction of a
582 bacterial flagellar chaperone FlgN with FlhA is required for efficient export of its
583 cognate substrates. *Mol. Microbiol.* 83, 775–788.
584 11. Kinoshita, M., Hara, N., Imada, K., Namba, K. & Minamino, T. (2013).
585 Interactions of bacterial flagellar chaperone-substrate complexes with FlhA
586 contribute to co-ordinating assembly of the flagellar filament. *Mol. Microbiol.*
587 90, 1249–1261.
588 12. Ibuki, T., Imada, K., Minamino, T., Kato, T., Miyata, T. & Namba, K. (2011).
589 Common architecture of the flagellar type III protein export apparatus and F-
590 and V-type ATPases. *Nat. Struct. Mol. Biol.* 18, 277–282

591 13. Kuhlen, L., Abrusci, P., Johnson, S., Gault, Deme, J., Caesar, J., Dietsche, T.,
592 Mebhratu, M. T., Ganief, T., Macek, B., Wagner, S., Robinson, C. V. & Lea, S.
593 M. (2018). Structure of the core of the type III secretion system export
594 apparatus. *Nat. Struct. Mol. Biol.* 25, 583-590.
595 14. Homma, M., Kutsukake, K., Iino, T. & Yamaguchi, S. (1984). Hook-associated
596 proteins essential for flagellar filament formation in *Salmonella* typhimurium. *J.*
597 *Bacteriol.* 157, 100-108.
598 15. Minamino, T. & Namba, K. (2008). Distinct roles of the FliI ATPase and proton
599 motive force in bacterial flagellar protein export. *Nature* 451, 485–488
600 16. Paul, K., Erhardt, M., Hirano, T., Blair, D. F. & Hughes, K. T. (2008). Energy
601 source of flagellar type III secretion. *Nature* 451, 489-492
602 17. Akeda, Y. & Galán, J. E. (2005). Chaperone release and unfolding of
603 substrates in type III secretion. *Nature* 437, 911–915.
604 18. Minamino, T., Morimoto, Y. V., Hara, N. & Namba, K. (2011). An energy
605 transduction mechanism used in bacterial flagellar type III protein export. *Nat.*
606 *Commun*. 2, 475
607 19. Lee, P. C., Zmina, S. E., Stopford, C. M., Toska, J. & Rietsch, A. (2014).
608 Control of type III secretion activity and substrate specificity by the cytoplasmic
609 regulator PcrG. *Proc. Natl. Acad. Sci. USA* 111, E2027–E2036.
610 20. Imada, K., Minamino, T., Kinoshita, M., Furukawa, Y. & Namba, K. (2010).
611 Structural insight into the regulatory mechanisms of interactions of the flagellar
612 type III chaperone FliT with its binding partners. *Proc. Natl. Acad. Sci. USA*
613 107, 8812–8817.
614 21. Yamamoto, S. & Kutsukake, K. (2006). FliT acts as an anti-$FlhD_2C_2$ factor in
615 the transcriptional control of the flagellar regulon in *Salmonella enterica*

616 serovar typhimurium. *J. Bacteriol.* 188, 6703–6708.
617 22. Kutsukake, K., Ikebe, T. & Yamamoto, S. (1999). Two novel regulatory genes,
618 fliT and fliZ, in the flagellar regulon of *Salmonella*. *Genes Genet. Syst.* 74,
619 287–292
620 23. Sato, Y., Takaya, A., Mouslim, C., Hughes, K. T. & Yamamoto, T. (2014). FliT
621 selectively enhances proteolysis of FlhC Subunit in $FlhD_4C_2$ complex by an
622 ATP-dependent protease, ClpXP. *J. Biol. Chem.* 289, 33001–33011
623 24. Fraser, G. M. & Hughes, C. (1999). Swarming motility. *Curr. Opin. Microbiol.* 2,
624 630-635.
625 25. Kearns, D. B. (2010). A field guide to bacterial swarming motility. *Nat. Rev.*
626 *Microbiol.* 8, 634-644
627 26. Dufour, A., Furness, R. B. & Hughes, C. (1998). Novel genes that upregulate
628 the *Proteus mirabilis* flhDC master operon controlling flagellar biogenesis and
629 swarming. *Mol. Microbiol.* 29, 741-751
630 27. Aldridge, P., Karlinsey. J. & Hughes, K. T. (2003). The type III secretion
631 chaperone FlgN regulates flagellar assembly via a negative feedback loop
632 containing its chaperone substrates FlgK and FlgL. *Mol. Microbiol.* 49, 1333-
633 1345
634 28. Hirano, T., Minamino, T., Namba, K. & Macnab, T. M. (2003). Substrate
635 specificity classes and the recognition signal for *Salmonella* type III flagellar
636 export. *J. Bacteriol.* 185, 2485-2492
637 29. Hughes, K. T., Gillen, K. L., Semon, M. J. & Karlinsey, J. E. (1993). Sensing
638 structural intermediates in bacterial flagellar assembly by export of a negative
639 regulator. *Science* 19, 1277-1280.
640 30. Kutsukake, K. (1994). Excretion of the anti-sigma factor through a flagellar

641 substructure couples flagellar gene expression with flagellar assembly in
642 *Salmonella* typhimurium. *Mol. Gen. Genet.* 15, 605-612
643 31. Lister, R., O'Malley, R. C., Tonti-Filippini, J., Gregory, D. B., Berry, C. C.,
644 Millar, A. H. & Ecker, J. R. (2008). Highly Integrated Single-Base Resolution
645 Maps of the Epigenome in *Arabidopsis*. *Cell* 133, 523-536
646 32. Mortazavi, A., Williams, B. A., McCue, K., Schaeffer, L. & Wold, B. (2008).
647 Mapping and quantifying mammalian transcriptomes by RNA-Seq. *Nat.*
648 *Methods* 5, 621-628
649 33. Nagalakshmi, U., Wang, Z., Waern, K., Shou, C., Raha, D., Gerstein, M. &
650 Synder, M. (2008). The transcriptional landscape of the yeast genome defined
651 by RNA sequencing. *Science* 320, 1344-1349.
652 34. Ingolia, N. T., Ghaemmaghami, S., Newman, J. R. & Weissman, J. S. (2009).
653 Genome-wide analysis in vivo of translation with nucleotide resolution using
654 ribosome profiling. *Science* 324, 218-223
655 35. Xing, Q., Shi, K., Portaliou, A., Rossi, P., Economou, A. & Kalodimos, C. G.
656 (2018). Structures of chaperone-substrate complexes docked onto the export
657 gate in a type III secretion system. *Nat. Commun.* 9, 1773.
658 36. Pallen, M. J., Bailey, C. M. & Beatson, S.A. (2006) Evolutionary links between
659 FliH/YscL-like proteins from bacterial type III secretion systems and second-
660 stalk components of the F_oF_1 and vacuolar ATPases. *Protein Sci*. 15, 935–
661 941.
662 37. Gledhill, J. R., Montgomery, M. G., Leslie, A. G. W. & Walker JE. (2007). How
663 the regulatory protein, IF1, inhibits F1-ATPase from bovine mitochondria. *Proc.*
664 *Natl. Acad. Sci. USA.* 104, 15671-15676.
665 38. Kato-Yamada, Y., Bald, D., Koike, M., Motohashi, K., Hisabori, T. & Yoshida, M.

666 (1999). ε Subunit, an endogenous inhibitor of bacterial F1-ATPase, also
667 inhibits F0F1-ATPase. *J. Biol. Chem.* 274, 33991-33994.
668 39. Yagi, H., Konno, H., Murakami-Fuse, T., Isu, A., Oroguchi, T., Akutsu, H.,
669 Ikeguchi, M. & Hisabori, T. (2009). Structural and functional analysis of the
670 intrinsic inhibitor subunit ε of F1 -ATPase from photosynthetic organisms.
671 *Biochem. J.* 425, 85-94.
672 40. Cherradi, Y., Hachani, A. & Allaoui, A. (2014). Spa13 of Shigella flexneri has a
673 dual role: chaperone escort and export gate-activator switch of the type III
674 secretion system. *Microbiology*. 160, 130-141.
675 41. Drehkopf, S., Otten, C., Hausner, J., Seifert, T. & Büttner, D. (2020). HrpB7
676 from Xanthomonas campestris pv. vesicatoria is an essential component of the
677 type III secretion system and shares features of HrpO/FliJ/YscO family
678 members. *Cell Microbiol.* 22, e13160.
679 42. Spöring, I., Felgner, S., Preuße, M., Eckweiler, D., Rohde, M., Häussler, M.,
680 Weiss, S. & Erhardt, M. (2018). Regulation of Flagellum Biosynthesis in
681 Response to Cell Envelope Stress in *Salmonella enterica* Serovar
682 Typhimurium. *MBio.* 9, e00736-17.
683 43. Adams, P., Fowler, R., Kinsella, N., Howell, G., Farris, M., Coote, P. &
684 O'connor, C. D. (2005). Proteomic detection of PhoPQ- and acid-mediated
685 repression of *Salmonella* motility. *Proteomics* 1, 597-607
686 44. Miao, E. A. & Rajan, J. V. (2011). *Salmonella* and Caspase-1: A complex
687 interplay of detection and evasion. *Front. Microbiol.* 2, 85.
688 45. Ilyas, B., Mulder, D. T., Little, D. J., Elhenawy, W., Banda, M. M., Perez-
689 Morales, D., Tsai, C. N., Chau, N. Y. E., Bustamante, V. H. & Coombes, B. K.
690 (2018). Regulatory Evolution Drives Evasion of Host Inflammasomes by

691 *Salmonella* Typhimurium. *Cell Rep.* 25, 825-832
692 46. Evans, L. D. B. & Hughes C. (2009). Selective binding of virulence type III
693 export chaperones by FliJ escort orthologues InvI and YscO. *FEMS Microbiol.*
694 *Lett.* 29, 292-297.
695 47. Cherradi, Y., Hachani, A. & Allaoui, A. (2014). Spa13 of *Shigella flexneri* has a
696 dual role: Chaperone escort and export gate-activator switch of the type III
697 secretion system. *Microbiology* 160, 130–141.
698 48. Yamaguchi, S., Fujita, H., Taira, T., Kutsukake, K., Homma, M. & Iino, T.
699 (1984). Genetic analysis of three additional fla genes in *Salmonella*
700 typhimurium. *J. Gen. Microbiol.* 130, 3339-3342
701 49. Hoffmann, S., Schmidt, C., Walter, S., Bender, J. K. & Gerlach, R. G. (2017).
702 Scarless deletion of up to seven methylaccepting chemotaxis genes with an
703 optimized method highlights key function of CheM in *Salmonella* Typhimurium.
704 *PLoS One* 12, e0172630.
705 50. Amann, E., Ochs, B. & Abel, K. J. (1988). Tightly regulated tac promoter
706 vectors useful for the expression of unfused and fused proteins in *Escherichia*
707 *coli*. *Gene* 69, 301-315.
708 51. Miroux, B. & Walker, J. E. (1996). Over-production of proteins in *Escherichia*
709 *coli*: Mutant hosts that allow synthesis of some membrane proteins and
710 globular proteins at high levels. *J. Mol. Biol.* 260, 289-298.
711 52. Thanabalu, T., Koronakis, E., Hughes, C. & Koronakis, V. (1998). Substrate-
712 induced assembly of a contiguous channel for protein export from *E.coli*:
713 reversible bridging of an inner-membrane translocase to an outer membrane
714 exit pore. *EMBO J.* 17, 6487-6496.
715 53. Kaelin, W. G., Krek, W., Sellers, W. R., DeCaprio, J. A., Ajchenbaum, F.,

716 Fuchs, C. S., Chittendan, T., Li, Y., Farnham, P. J., Blanar, M. A., Livingston,
717 D. M. & Flemington, E. K. (1992). Expression cloning of a cDNA encoding a
718 retinoblastoma-binding protein with E2F-like properties. *Cell* 70, 351-364
719 54. Chung, B. Y. W., Deery, M. J., Groen, A. J., Howard, J. & Baulcombe, D. C.
720 (2017). Endogenous miRNA in the green alga *Chlamydomonas* regulates gene
721 expression through CDS-targeting. *Nat Plants* 3, 787-794
722 55. Chung, B.Y. W., Hardcastle, T. J., Jones, J. D., Irigoyen, N., Firth, A. E.,
723 Baulcombe, D. C. & Brierley, I. (2015). The use of duplex-specific nuclease in
724 ribosome profiling and a user-friendly software package for Ribo-seq data
725 analysis. *RNA* 21, 1731-1745
726 56. Hardcastle, T. J. (2015). Data from “Analysis of sequencing data from ribosome
727 profiling experiments.” Bioconductor. Available at
728 doi:10.18129/B9.bioc.riboSeqR.
729
730

731 **Figure Legends**

732 **Figure 1 Identification of chaperone variants defective for FliJ binding**

733 **A.** Atomic resolution structure of the 140-residue *Salmonella* FlgN (PDB: 5B3D)
734 indicating the region (residues 70-102; red) in which three-residue scanning
735 deletions were introduced.

736

737 **B.** Affinity chromatography of glutathione sepharose-bound GST-FliJ or GST-FlgK
738 incubated with cell lysates containing wild type FlgN or its three-amino acid deletion
739 variants. After washing, proteins were eluted in SDS-loading buffer, separated by
740 SDS(15%)-PAGE and stained with Coomassie Brilliant Blue. Apparent molecular
741 weights are in kilodaltons (kDa).

742

743 **C.** Affinity chromatography of glutathione sepharose-bound GST-FliJ, GST-FlgK or
744 GST-FlhA$_C$ incubated with cell lysates containing wild type FlgN or its derivative
745 variants FlgNΔ76-78, FlgN-W78A or FlgNΔ90-100. After washing, proteins were
746 eluted in SDS-loading buffer, separated by SDS(15%)-PAGE and stained with
747 Coomassie Brilliant Blue. Apparent molecular weights are in kilodaltons (kDa).

748

749 **D.** Atomic resolution structure of the 122-residue *Salmonella* FliT (PDB: 3A7M)
750 indicating the position of conserved residues (red) within the region essential for FliJ
751 binding. *In vitro* binding to FliJ is enhanced by truncating FliT at residue 94 (dashed
752 red line).

753

754 **E.** Affinity chromatography of glutathione sepharose-bound GST-FliJ with cell lysates
755 containing FliT94 or its point mutant variants. After washing, proteins were eluted in

756 SDS-loading buffer, separated by SDS(15%)-PAGE and stained with Coomassie
757 Brilliant Blue. Apparent molecular weights are in kilodaltons (kDa).
758
759 **F.** Affinity chromatography of glutathione sepharose-bound GST-FlhA$_C$ incubated
760 with cell lysates containing FliD and wild type FliT or its point mutant variants FliT-
761 L72A or FliT-Y106A. After washing, proteins were eluted in SDS-loading buffer,
762 separated by SDS(15%)-PAGE and stained with Coomassie Brilliant Blue (top panel)
763 or were analysed by immunoblotting with anti-FliT or anti-FliD polyclonal antisera
764 (middle and bottom panels). Apparent molecular weights are in kilodaltons (kDa).
765
766 **Figure 2 FliJ binding to FlgN and FliT is required for efficient cell motility and**
767 **subunit export**
768 **A.** Swimming (top panel; 0.25% soft tryptone agar) and swarming (bottom panels;
769 0.6% agar-tryptone with 0.5% glucose) motility of recombinant *Salmonella* strains
770 producing chromosomally-encoded FlgN variants (W78A, Δ76-78, or Δ90-100), the
771 SJW1103 wild type, and the *Salmonella flgN* null strain (Δ*flgN*).
772
773 **B.** Whole cell (cell) and supernatant (secreted) proteins from late exponential-phase
774 cultures of *Salmonella* strains producing chromosomally-encoded FlgN variants
775 (W78A, Δ76-78, or Δ90-100), the SJW1103 wild type, and the *Salmonella flgN* null
776 strain (Δ*flgN*) were separated by SDS (15%)-PAGE and analysed by immunoblotting
777 with anti-FliC, anti-FlgK or anti-FlgN polyclonal antisera. Apparent molecular weights
778 are in kilodaltons (kDa).
779

780 **C.** Swimming (top panel; 0.25% soft tryptone agar) and swarming (bottom panels;
781 0.6% agar-tryptone with 0.5% glucose) motility of recombinant *Salmonella* strains
782 producing chromosomally-encoded FliT variants (L72A and Y106A), the SJW1103
783 wild type, and the *Salmonella fliT* null strain (Δ*fliT*).
784
785 **D.** Whole cell (cell) and supernatant (secreted) proteins from late exponential-phase
786 cultures of *Salmonella* strains producing chromosomally-encoded FliT variants (L72A
787 and Y106A), the SJW1103 wild type, and the *Salmonella fliT* null strain (Δ*fliT*) were
788 separated by SDS (15%)-PAGE and analysed by immunoblotting with anti-FliC, anti-
789 FliD or anti-FliT polyclonal antisera. Apparent molecular weights are in kilodaltons
790 (kDa).
791
792 **Figure 3 FlgN and FliT chaperones compete with $FlhA_C$ for binding to FliJ *in***
793 ***vitro*.**
794 **A.** *In vitro* competition assay to assess $FlhA_C$ binding to cobalt (Co^{2+}) bead-
795 immobilized $(His)_6$-FliJ in the presence of the FlgN or FliT chaperones, or chaperone
796 variants that cannot bind FliJ (FliJ non-binder).
797
798 **B.** Cell lysates of *E.coli* C41 expressing FliT94, which cannot bind $FlhA_C$ (-), or its
799 L72A variant, which cannot bind $FlhA_C$ or FliJ (left-hand panels), or FlgN Y112A
800 which cannot bind $FlhA_C$ (-) or its Δ76-78 variant, which cannot bind $FlhA_C$ or FliJ
801 (right-hand panels) were mixed with *E.coli* C41 lysates containing $FlhA_C$ (load) and
802 incubated with cobalt bead-immobilized $(His)_6$-FliJ (bound). After washing, proteins
803 were eluted from the cobalt beads in SDS-loading buffer, separated by SDS(15%)-

804 PAGE and analysed by immunoblotting with anti-FlhA, anti-FliT, anti-FlgN or anti-FliJ
805 polyclonal antisera. Apparent molecular weights are in kilodaltons (kDa).
806
807 **Figure 4 FlgN and FliT chaperones compete with $FlhA_C$ for binding to FliJ *in*
808 *vivo*.**
809 **A.** *In vivo* competition assay to assess the effect of chaperone-FliJ binding on $FlhA_C$
810 export activity. Export of the unchaperoned FlgD subunit was assessed in a *flgE* null
811 strain. Whole cell (cell) and supernatant (secreted) proteins from late exponential-
812 phase cultures of *Salmonella* Δ*flgE* strains producing pTrc99a-encoded FlgN Y122A
813 (-) or FlgN Y122A, Δ76-78 (Δ76-78) were separated by SDS (15%)-PAGE and
814 analysed by immunoblotting with anti-FlgD, anti-FlgN, anti-FliJ and anti-FlhA
815 polyclonal antisera. Apparent molecular weights are in kilodaltons (kDa). Relative
816 amounts of FlgD secreted into culture supernatants were quantified using image
817 Studio Lite software and normalized to FlgD secreted by cells expressing the FlgN
818 Δ76-78 Y122A variant (right-hand bar chart). Export of non-cognate subunit FlgD is
819 attenuated in cells producing FlgN Y122A (-), which binds FliJ but not FlhA, but is
820 significantly higher in cells producing the FlgN variant defective in binding FliJ (FlgN
821 Δ76-78,Y122A). Data shown are the mean ± SEM of three biological replicates.
822 *Statistically significant difference, p <0.01 (unpaired two-tailed t-test).
823
824 **Figure 5 Ribosome profiling reveals cytoplasmic ratios of flagellar subunits to
825 their cognate chaperones**
826 **A.** Smoothed scatter plot of total translation (Ribosome profiling, measurement of
827 ribosome occupation) and total mRNA abundance (RNA-Seq), showing flagellar

828 chaperones FlgN, FliT and FliS (blue), their respective cognate subunits (red), and
829 the regression between total translation and mRNA abundance (dotted line).
830
831 **B.** Ratios of the normalised translation to gene length for the coding regions
832 corresponding to chaperones and their cognate subunits (FlgN:FlgK+FlgL; FliT:FliD;
833 FliS:FliC).
834
835 **Figure 6 Chaperone regulation of the fT3SS machinery in response to subunit**
836 **cargo availability**
837 Chaperone-subunit complexes initially dock at the FliI component of the ATPase
838 complex (1) before docking at the cytoplasmic domain of FlhA (2). Subunits are
839 subsequently released from their cognate chaperones and translocated into the
840 export channel (3). Unladen chaperones then bind FliJ from which they are captured
841 by newly synthesized cognate subunits (4). Chaperone-subunit complexes
842 subsequently dock at the FliI component of the ATPase, repeating the cycle (5).
843 Under conditions where subunit availability is limited (right-hand panel), unladen
844 FlgN and FliT chaperones remain bound to FliJ, blocking the interaction of FliJ with
845 FlhA and reducing pmf-driven export by the fT3SS machinery.
846
847 **Supplementary Figure Legends**
848 **Figure S1.**
849 **A**. Affinity chromatography of glutathione sepharose-bound glutathione-S-
850 transferase (GST) incubated with cell lysates containing FliT94. After washing,
851 proteins were eluted in SDS-loading buffer, separated by SDS(15%)-PAGE and
852 stained with Coomassie Brilliant Blue (top panel). The cell lysate load was analyzed

853 by immunoblotting with polyclonal anti-FliT anti-sera (bottom panel). Apparent
854 molecular weights are in kilodaltons (kDa).
855
856 **B**. Affinity chromatography of glutathione sepharose-bound glutathione-S-
857 transferase (GST) incubated with cell lysates containing FlgN. After washing,
858 proteins were eluted in SDS-loading buffer, separated by SDS(15%)-PAGE and
859 stained with Coomassie Brilliant Blue (top panel). The cell lysate load was analyzed
860 by immunoblotting with polyclonal anti-FlgN anti-sera (bottom panel). Apparent
861 molecular weights are in kilodaltons (kDa).
862
863 **Figure S2.**
864 **A**. Affinity chromatography of glutathione sepharose-bound GST-FlgL (top two
865 panels) or glutathione-S-transferase (GST; bottom panels) incubated with cell
866 lysates containing FlgN or its derivative variants FlgNΔ76-78, FlgN-W78A or
867 FlgNΔ90-100. After washing, proteins were eluted in SDS-loading buffer, separated
868 by SDS(15%)-PAGE and stained with Coomassie Brilliant Blue to visualise GST-
869 FlgL and GST, or analysed by immunoblotting with polyclonal anti-FlgN anti-sera.
870 The cell lysate load (FlgN load) was also analyzed by immunoblotting with polyclonal
871 anti-FlgN anti-sera. Apparent molecular weights are in kilodaltons (kDa).
872
873 **B**. Affinity chromatography of glutathione sepharose-bound GST-FliJ (top two
874 panels), GST-FliD (middle two panels) or glutathione-S-transferase (GST; bottom
875 panels) with cell lysates containing FliT and its mutant variants. After washing,
876 proteins were eluted in SDS-loading buffer, separated by SDS(15%)-PAGE and
877 stained with Coomassie Brilliant Blue to visualise GST-FliJ, GST-FliD and GST, or

878 analysed by immunoblotting with polyclonal anti-FliT anti-sera. The cell lysate load
879 (FliT load) was also analyzed by immunoblotting with polyclonal anti-FliT anti-sera.
880 Apparent molecular weights are in kilodaltons (kDa).
881
882 **C**. Cell lysates of *E.coli* C41 expressing FliT (top panel) or FliD (bottom panel) used
883 as load fractions in affinity chromatography assays with GST-FlhA$_C$ in Figure 1.
884 Proteins were separated by SDS(15%)-PAGE and analysed by immunoblotting with
885 polyclonal anti-FliT anti-sera or polyclonal anti-FliD anti-sera.
886
887 **Figure S3.**
888 **A**. Whole cell and supernatant proteins from late exponential-phase cultures of
889 *Salmonella* strains producing chromosomally-encoded FliT variants (L72A and
890 Y106A), the *Salmonella fliT* null strain (Δ*fliT*), and the SJW1103 wild type were
891 separated by SDS (15%)-PAGE and analysed by immunoblotting with anti-FlgK
892 polyclonal antisera. Apparent molecular weights are in kilodaltons (kDa).
893
894 **Figure S4.**
895 **A.** Whole cell proteins from late exponential-phase cultures of a *Salmonella flgD* null
896 strain (Δ*flgD*), and the SJW1103 wild type were separated by SDS (15%)-PAGE and
897 analysed by immunoblotting with anti-FlgK polyclonal antisera. Apparent molecular
898 weights are in kilodaltons (kDa).
899
900

FIGURE 1

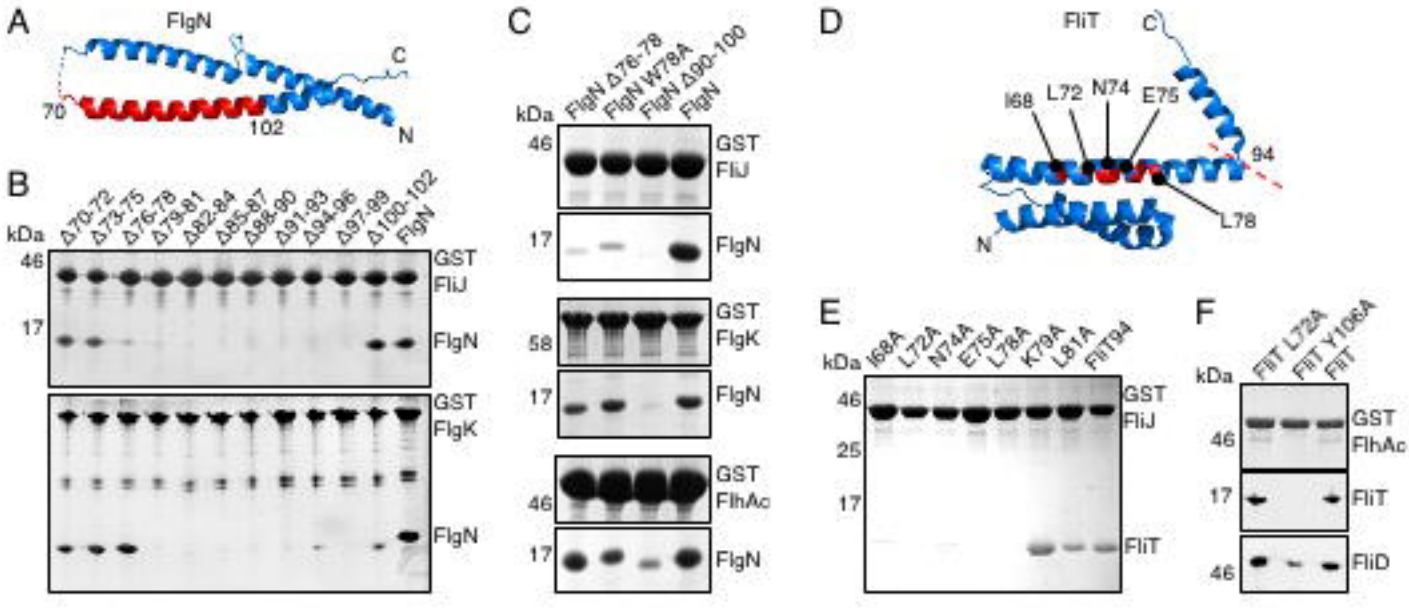
A
FlgN
C
70
102
N
B
kDa
Δ70-72
Δ73-75
Δ76-78
Δ79-81
Δ82-84
Δ85-87
Δ88-90
Δ91-93
Δ94-96
Δ97-99
Δ100-102
FlgN
46
17
GST
FliJ
FlgN
GST
FlgK
FlgN
C
FlgN Δ76-78
FlgN W79A
FlgN Δ90-100
FlgN
kDa
46
GST
FliJ
17
FlgN
58
GST
FlgK
17
FlgN
46
GST
FlhAc
17
FlgN
D
FliT
C
I68
L72
N74
E75
94
L78
N
E
kDa
I68A
L72A
N74A
E75A
L78A
K79A
L81A
FliT94
46
25
17
GST
FliJ
FliT
F
kDa
FliT L72A
FliT Y106A
FliT
46
GST
FlhAc
17
FliT
46
FliD

FIGURE 2

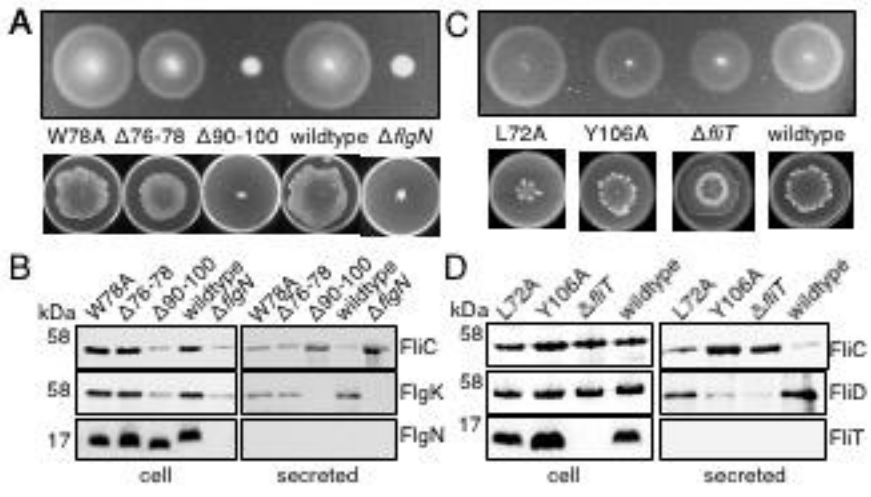
A
W78A Δ76-78 Δ90-100 wildtype ΔflgN
C
L72A Y106A ΔfliT wildtype
B
kDa W78A Δ76-78 Δ90-100 wildtype ΔflgN W78A Δ76-78 Δ90-100 wildtype ΔflgN
58
58
17
FliC
FlgK
FlgN
cell
secreted
D
kDa L72A Y106A ΔfliT wildtype L72A Y106A ΔfliT wildtype
58
58
17
FliC
FliD
FliT
cell
secreted

FIGURE 3

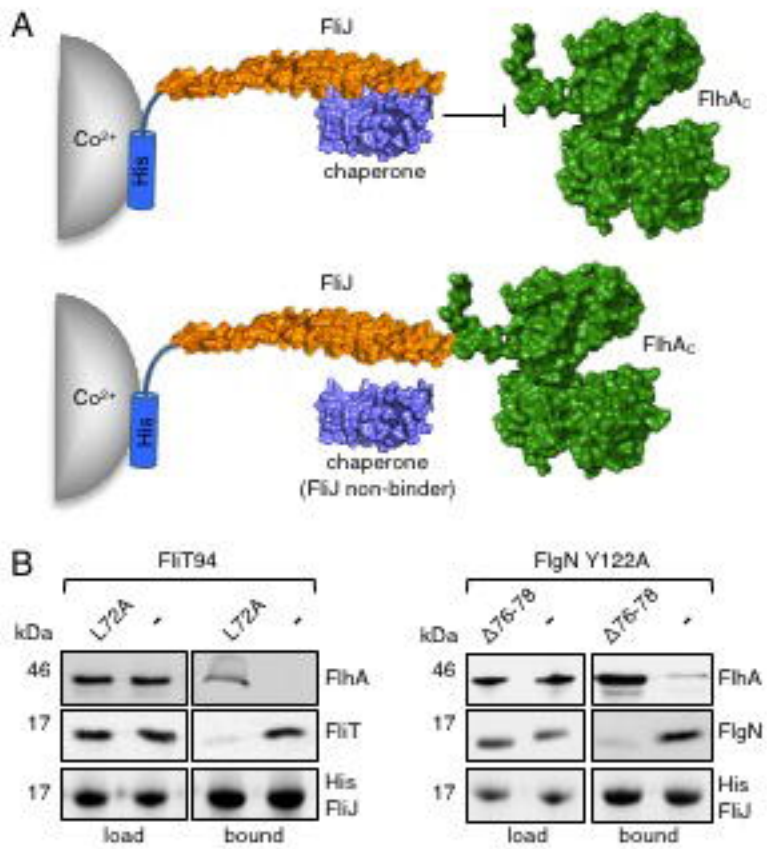
A
FliJ
Co2+
His
chaperone
FlhAC
FliJ
Co2+
His
chaperone
(FliJ non-binder)
FlhAC
B
FliT94
L72A
-
L72A
-
kDa
46
17
17
FlhA
FliT
His
FliJ
load
bound
FlgN Y122A
Δ76-78
-
Δ76-78
-
kDa
46
17
17
FlhA
FlgN
His
FliJ
load
bound

FIGURE 4

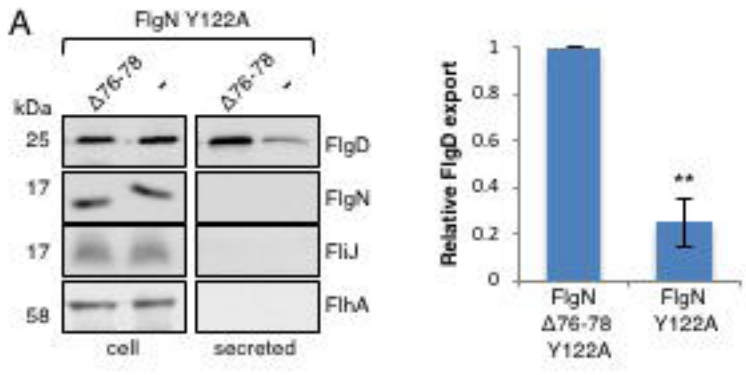
A
FlgN Y122A
Δ76-78
Δ76-78
kDa
25
17
17
58
FlgD
FlgN
FliJ
FlhA
cell
secreted
Relative FlgD export
1
0.8
0.6
0.4
0.2
0
**
FlgN Δ76-78 Y122A
FlgN Y122A

FIGURE 5

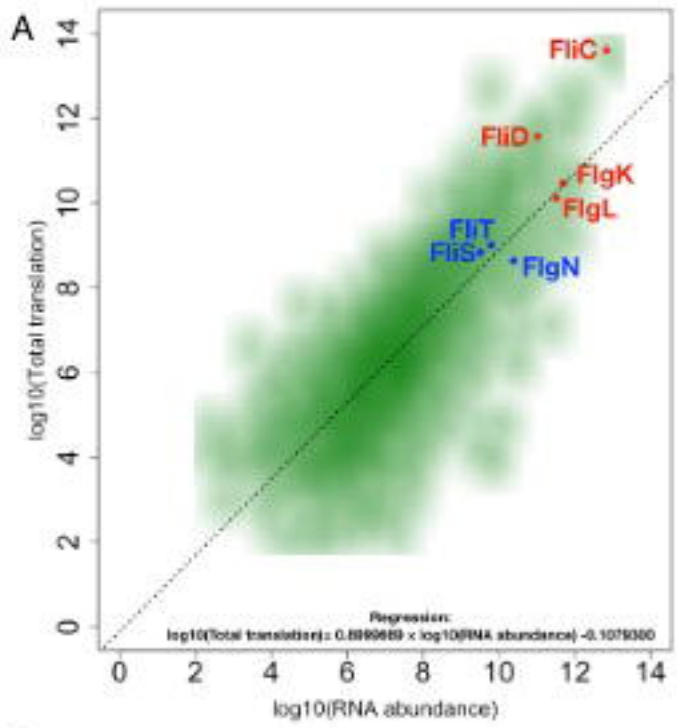
A
FliC
FliD
FlgK
FlgL
FlIT
FliS
FlgN
log10(Total translation)
log10(RNA abundance)
0
2
4
6
8
10
12
14

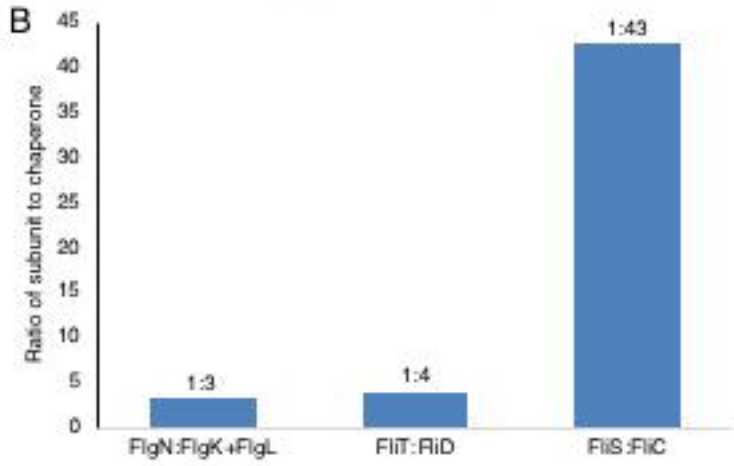
B
Ratio of subunit to chaperone
45
40
35
30
25
20
15
10
5
0
1:3
1:4
1:43
FlgN:FlgK+FlgL
FlIT:FliD
FliS:FliC

FIGURE 6

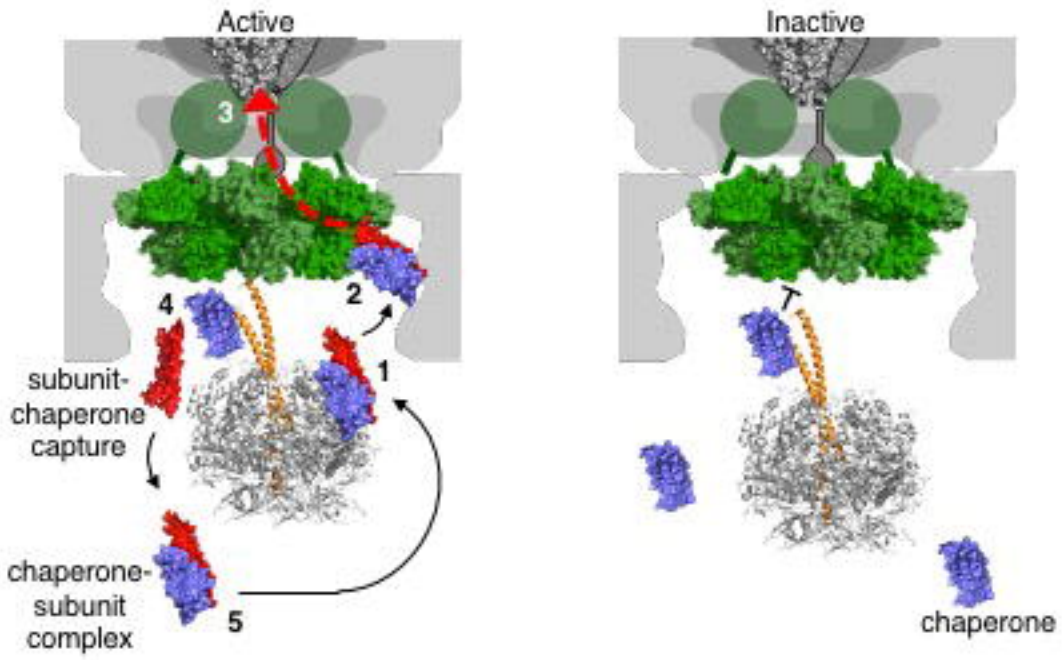
Active
Inactive
3
2
4
1
subunit-
chaperone
capture
chaperone-
subunit
complex
5
chaperone